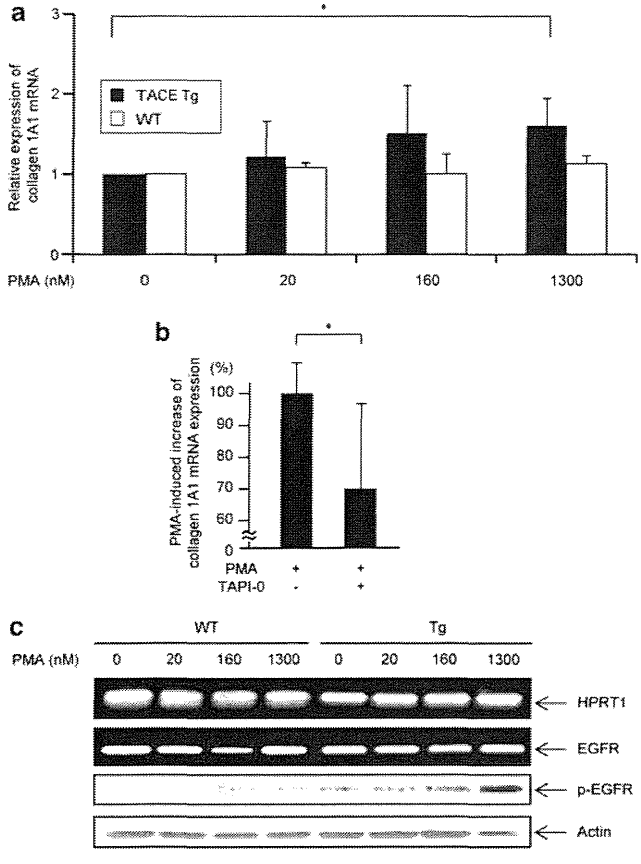

Figure 7 Increased type I collagen and phosphorylated EGFR in fibroblasts by PMA. The primary culture of dermal fibroblasts (TACE-Tg: $n=3$, WT: $n=3$) was treated by PMA at respective concentrations of 0, 20, 160, and 1300 nM. After 4 h of incubation at 37 °C, RNA was extracted from the cells, and then the expression of type I collagen (collagen 1A1) was examined by real-time RT-PCR (**a**). The fibroblasts derived from TACE-Tg mice were treated by 1300 nM of PMA with or without 25 μg/ml of TAPI-0 at 37 °C. After 4 h of incubation, RNA was extracted from the cells, and then the expression of type I collagen (collagen 1A1) was examined by real-time RT-PCR (**b**). The PMA-induced increase of type I collagen (collagen 1A1) was set as 100%. *$P<0.05$. To determine the activation of EGFR, the expressions of EGFR and phosphorylated EGFR were examined (**c**). The primary culture of dermal fibroblasts was treated by PMA at respective concentrations of 0, 20, 160, and 1300 nM. After 1 h of incubation at 37 °C, RNA and cell lysates were extracted. The RNA was served for RT-PCR using the HPRT1 and EGFR primers. The lysates adjusted ranging from 10 to 40 μg/lane were fractionated on 7.5% SDS polyacrylamide gel, and then transferred onto PVDF membranes. After blocking by TBS-T containing 1% nonfat milk, the membranes were incubated with 1:2500 dilution of the anti-phosphorylated EGFR (p-EGFR) antibody overnight at 4 °C. After 3 times of wash by TBS-T, the membranes were next incubated with 1:25 000 dilution of the peroxidase-labeled secondary antibodies overnight at 4 °C. Protein bands were detected using ECL Advance Western Blotting Detection kit. As an internal control, the amount of actin was monitored by the anti-actin antibody. Experiments were repeated 3 times, and similar results were reproduced. Representative data are shown.

collagen using primary culture of dermal fibroblasts was examined in this study. Results indicated that PMA effectively activated TACE and subsequently increased expression of the type I collagen in the fibroblasts derived from TACE-Tg mice (Figure 7a). Furthermore, the induction of type I collagen by PMA was significantly inhibited by the TACE inhibitor (Figure 7b). These findings support our conclusion that TACE overexpression and activation in fibroblasts could contribute to dermal fibrosis. However, this does not necessarily mean that TACE exclusively regulates the PMA-induced type I collagen expression in dermal fibroblasts because TAPI-0 is not a specific inhibitor of TACE.

The substrates of TACE involved in the process of dermal fibrosis after the PMA-induced inflammation have not been identified. However, the amount of phosphorylated EGFR was increased by the PMA treatment of dermal fibroblasts (Figure 7c). As the expression of type I collagen could be driven by the EGFR signal,[12] TACE activated by PMA could shed off putative EGFR ligands on the surface of fibroblasts. Subsequently, the soluble EGFR ligands could bind and activate EGFR on fibroblasts through the autocrine and paracrine pathways and increase the type I collagen expression resulting in induction of dermal fibrosis. With regard to the EGF signaling pathway, EGFR ligands, including transforming growth factor-α (TGF-α), heparin-binding EGF (HB-EGF), amphiregulin, and epiregulin, may be the candidates shed by TACE. Among them, amphiregulin is known to be expressed in fibroblasts;[19] thus, this molecule is the next target in our continuing study.

The EGFR expression has been reported to be upregulated in dermal fibroblasts of SSc patients.[20] In the present study, the EGFR expression in TACE-Tg-derived dermal fibroblasts did not appear to be increased by PMA *in vitro*. This could be interpreted by the short duration of PMA stimulation (1 h stimulation) in the experiments. In addition, murine bleomycin-induced lung fibrosis could be suppressed by the EGFR tyrosine kinase inhibitor.[21] These findings suggest that the EGF signaling pathway comes to a great interest as the mechanism bridging the TACE expression and the pathogenesis of fibrosis.

In summary, the collective findings suggest the possibility that overexpression of TACE in fibroblasts could contribute to the pathogenesis of dermal fibrosis after inflammation. Further studies are needed to reveal the process leading to fibrosis; however, our data suggest that TACE and EGFR on fibroblasts may be novel therapeutic targets of dermal fibrosis, which is induced after diverse inflammatory disorders of the skin.

Supplementary Information accompanies the paper on the Laboratory Investigation website (http://www.laboratoryinvestigation.org)

DISCLOSURE/CONFLICT OF INTEREST

The authors declare no conflict of interest.

1. Black RA, Rauch CT, Kozlosky CJ, *et al.* A metalloproteinase disintegrin that releases tumour-necrosis factor-α from cells. Nature 1997;385: 729–733.

2. Moss ML, Jin SL, Milla ME, *et al.* Cloning of a disintegrin metalloproteinase that processes precursor tumour-necrosis factor-α. Nature 1997;385:733–736.
3. Van Wart HE, Birkedal-Hansen H. The cysteine switch: a principle of regulation of metalloproteinase activity with potential applicability to the entire matrix metalloproteinase gene family. Proc Natl Acad Sci USA 1990;87:5578–5582.
4. Grams F, Huber R, Kress LF, *et al.* Activation of snake venom metalloproteinases by a cysteine switch-like mechanism. FEBS Lett 1993;335:76–80.
5. Kang T, Zhao YG, Pei D, *et al.* Intracellular activation of human adamalysin 19/disintegrin and metalloproteinase 19 by furin occurs via one of the two consecutive recognition sites. J Biol Chem 2002;277:25583–25591.
6. Endres K, Anders A, Kojro E, *et al.* Tumor necrosis factor-α converting enzyme is processed by proprotein-convertases to its mature form which is degraded upon phorbol ester stimulation. Eur J Biochem 2003;270:2386–2393.
7. Doggrell SA. TACE inhibition: a new approach to treating inflammation. Expert Opin Investig Drugs 2002;11:1003–1006.
8. Shimizu M, Hasegawa N, Nishimura T, *et al.* Effects of TNF-α-converting enzyme inhibition on acute lung injury induced by endotoxin in the rat. Shock 2009;32:535–540.
9. Terao M, Murota H, Kitaba S, *et al.* Tumor necrosis factor-α processing inhibitor-1 inhibits skin fibrosis in a bleomycin-induced murine model of scleroderma. Exp Dermatol 2010;19:38–43.
10. Mohler KM, Sleath PR, Fitzner JN, *et al.* Protection against a lethal dose of endotoxin by an inhibitor of tumour necrosis factor processing. Nature 1994;370:218–220.
11. Maltzan K, Tan W, Pruett SB. Investigation of the role of TNF-α converting enzyme (TACE) in the inhibition of cell surface and soluble TNF-α production by acute ethanol exposure. PLoS One 2012;7:e29890.
12. Wu D, Peng F, Zhang B. Collagen I induction by high glucose levels is mediated by epidermal growth factor receptor and phosphoinositide 3-kinase/Akt signalling in mesangial cells. Diabetologia 2007;50: 2008–2018.
13. Ohta S, Harigai M, Tanaka M, *et al.* Tumor necrosis factor-α (TNF-α) converting enzyme contributes to production of TNF-α in synovial tissues from patients with rheumatoid arthritis. J Rheumatol 2001;28:1756–1763.
14. Moss ML, Sklair-Tavron L, Nudelman R. Drug insight: tumor necrosis factor-converting enzyme as a pharmaceutical target for rheumatoid arthritis. Nat Clin Pract Rheumatol 2008;4:300–309.
15. Bohgaki T, Amasaki Y, Nishimura N, *et al.* Up regulated expression of tumour necrosis factor α converting enzyme in peripheral monocytes of patients with early systemic sclerosis. Ann Rheum Dis 2005;64:1165–1173.
16. Leco KJ, Waterhouse P, Sanchez OH, *et al.* Spontaneous air space enlargement in the lungs of mice lacking tissue inhibitor of metalloproteinases-3 (TIMP-3). J Clin Invest 2001;108:817–829.
17. Mohammed FF, Smookler DS, Taylor SE, *et al.* Abnormal TNF activity in $Timp3^{-/-}$ mice leads to chronic hepatic inflammation and failure of liver regeneration. Nat Genet 2004;36:969–977.
18. Smookler DS, Mohammed FF, Kassiri Z, *et al.* Tissue inhibitor of metalloproteinase 3 regulates TNF-dependent systemic inflammation. J Immunol 2006;176:721–725.
19. Torring N, Sorensen BS, Bosch ST, *et al.* Amphiregulin is expressed in primary cultures of prostate myofibroblasts, fibroblasts, epithelial cells, and in prostate tissue. Prostate Cancer Prostatic Dis 1998;1:262–267.
20. Tokiyama K, Yokota E, Niho Y. Epidermal growth factor receptor of fibroblasts from patients with scleroderma. J Rheumatol 1990;17: 1463–1468.
21. Wang P, Tian Q, Liang ZX, *et al.* Gefitinib attenuates murine pulmonary fibrosis induced by bleomycin. Chin Med J (Engl) 2010;123:2259–2264.

RHEUMATOLOGY

Rheumatology 2013;52:523–528
doi:10.1093/rheumatology/kes310
Advance Access publication 28 November 2012

Concise report

Positive synovial vascularity in patients with low disease activity indicates smouldering inflammation leading to joint damage in rheumatoid arthritis: time-integrated joint inflammation estimated by synovial vascularity in each finger joint

Jun Fukae[1], Masato Isobe[1], Akemi Kitano[1], Mihoko Henmi[1], Fumihiko Sakamoto[1], Akihiro Narita[1], Takeya Ito[1], Akio Mitsuzaki[1], Masato Shimizu[1], Kazuhide Tanimura[1], Megumi Matsuhashi[1], Tamotsu Kamishima[2], Tatsuya Atsumi[3] and Takao Koike[3]

Abstract

Objective. To investigate the relationship between synovial vascularity and joint damage progression in each finger joint of patients with RA under low disease activity during treatment with biologic agents.

Methods. We studied 310 MCP and 310 PIP joints of 31 patients with active RA who were administered adalimumab (ADA) or tocilizumab (TCZ). Patients were examined with clinical and laboratory assessments. Power Doppler sonography was performed at baseline and at weeks 8, 20 and 40. Synovial vascularity was evaluated according to quantitative measurement. Hand and foot radiography was performed at baseline and at week 50.

Results. Composite scores of the DAS with 28 joints and the Simplified Disease Activity Index (SDAI) were significantly decreased from baseline to week 8, being sustained at a low level by biologic agents during the observational period. MCP and PIP joints with positive synovial vascularity after week 8 showed more subsequent joint damage progression than joints without synovial vascularity throughout the follow-up. The changes in radiographic progression in these joints were independent of the sum of synovial vascularity from baseline to week 40 or the occasional occurrence of positive synovial vascularity.

Conclusion. Smouldering inflammation reflected by positive synovial vascularity under low disease activity was linked to joint damage. The damage progressed irrespective of the severity of positive synovial vascularity. Even with a favourable overall therapeutic response, monitoring of synovial vascularity has the potential to provide useful joint information to tailor treatment strategies.

Trial registration. University Hospital Medical Information Network Clinical Trials Registry; http://www.umin.ac.jp/ctr/; UMIN000004476.

Key words: rheumatoid arthritis, power Doppler sonography, synovial vascularity, low disease activity.

CLINICAL

[1]Hokkaido Medical Center for Rheumatic Diseases, [2]Faculty of Health Science, Hokkaido University Graduate School of Health Science and, [3]Department of Medicine II, Hokkaido University Graduate School of Medicine, Sapporo, Japan.

Submitted 31 July 2012; revised version accepted 27 September 2012.

Correspondence to: Jun Fukae, Hokkaido Medical Center for Rheumatic Diseases, 1-45, 3-Chome, 1-Jo, Kotoni, Nishi-ku, Sapporo 063-0811, Japan. E-mail: jun.fukae@ryumachi-jp.com

Introduction

In RA, clinical evaluations for disease activity such as patients' symptoms, joint examinations and laboratory data do not have enough power to provide details on local joint inflammation [1]. To assess rheumatoid disease activity, composite scores such as the ACR core data set or the DAS with 28 joints (DAS28) have been developed to

compensate for the weak points in the use of a single clinical marker [2, 3]. Although these composite scores have been well established as disease activity markers, they cannot precisely predict the destruction of individual joints.

The appearance and increase in synovial vascularity related to vasodilation and angiogenesis indicates active joint inflammation [4]. Power Doppler sonography (PDS) enables visualization of synovial vascularity and numerical representation of local inflammation [5, 6].

We focused on the clinical significance of synovial vascularity in RA. We previously reported the prediction of the progression of local finger joint damage via early changes in synovial vascularity [7, 8]. Interestingly, we observed finger joints with persistence of synovial vascularity after achieving low disease activity. Here we report on the relationship between synovial vascularity and joint damage progression in two patient groups treated with different biologic agents, focusing on finger joints with positive synovial vascularity after achieving low disease activity.

Patients and methods

Patients

Thirty-one patients with RA who had started adalimumab (ADA) or tocilizumab (TCZ) therapies were analysed. The patients had been pre-treated with DMARDs [ADA: eight patients with MTX, one with tacrolimus (TAC), one with bucillamine (BUC) + TAC, one with MTX + TAC and one with SSZ + TAC; TCZ: nine patients with MTX, one with BUC and two with TAC] or pre-treated with biologic agents [ADA: one patient with MTX + infliximab (IFX); TCZ: three patients with MTX + IFX, one with MTX + etanercept and two with MTX + ADA]. Despite these treatment histories, all patients were refractory cases having at least one swollen joint in the MCP/PIP joints and a DAS28-ESR > 3.2. Demographic, clinical and laboratory characteristics of the patients are shown in Table 1. After baseline examinations, ADA was given to 13 patients and TCZ to 18 patients. The biologic agents were given according to the standard protocols (ADA 40 mg s.c. injection bi-weekly, TCZ 8 mg/kg i.v. infusion every 4 weeks). This study was conducted in accordance with the Declaration of Helsinki and was approved by the local ethics committee of Hokkaido Medical Center for Rheumatic Diseases. Informed consent was obtained from all patients before they entered the study.

Clinical examination

Swollen and tender joints and global assessment on a visual analogue scale (VAS) were assessed at baseline and at weeks 8, 20 and 40 by rheumatologists (J.F., M.S., M.M., K.T.) who were blinded to the ultrasonographic results. Blood tests for ESR and CRP were performed at each assessment.

Ultrasonography and assessment

Ultrasonography was performed at baseline and at weeks 8, 20 and 40 by one of three US experts (M.H., F.S., A.N.) specialized in musculoskeletal ultrasonography who were blinded to other clinical information. A linear array transducer (13 MHz) and ultrasonographic machine were used (EUP-L34P, EUB-7500, Hitachi, Tokyo, Japan). Power Doppler settings have been previously described [7, 8]. First to fifth MCP and first to fifth PIP joints were scanned in the longitudinal plane over the dorsal surface. The quantitative PDS method was established in a previous report [8]. A value of synovial vascularity was determined by counting the number of vascular flow pixels in the region of interest.

Radiography and assessment

Plain radiographs of hands, wrists and feet were obtained at baseline and at week 50. Radiological assessments were examined according to the Genant-modified Sharp score (GSS) by a rheumatologist (M.S.) who was blinded to other clinical information [9].

Statistical analysis

Differences of composite parameters were examined using the Student's *t*-test and other data were examined using a non-parametric test (Wilcoxon's signed-rank test and Mann–Whitney U test). Intra- and interobserver reliability of quantitative PDS were estimated by intraclass correlation coefficients (ICCs). The smallest detectable change for the radiographic score change was calculated according to a previous study [10]. $P < 0.05$ indicated statistical significance. Statistical analyses were calculated with the use of Excel (Microsoft, Redmond, WA, USA) and MedCalc 12.1.4.0 (MedCalc Software, Mariakerke, Belgium).

Results

Clinical disease activity

At baseline there were no significant differences of DAS28-ESR and SDAI between the ADA and TCZ groups (Table 1). In both groups these parameters were significantly decreased from baseline to week 8, followed by sustained low disease activity (ADA: $P = 0.0007$, $P = 0.0005$; TCZ: $P < 0.0001$, $P < 0.0001$, respectively) (Table 1).

Radiographic evaluation of joint damage

At baseline there were no significant differences in total GSS (TGSS) between the ADA and TCZ groups (Table 1). In both groups the TGSS increased significantly from baseline to week 50 ($P = 0.0122$, $P = 0.0181$, respectively).

Local GSS (LGSS) was evaluated in each finger joint. In the ADA group the median of the LGSS at baseline for MCP and PIP joints was 2 [interquartile range (IQR) 2–4] and 3 (IQR 1.5–4), respectively, and in the TCZ group the median of the LGSS at baseline for MCP and PIP joints was 3 (IQR 2–4) and 3 (IQR 2–4), respectively. The smallest detectable change values was calculated for the LGSS for single MCP and PIP joints [0.33, 0.31 less than the smallest unit of GSS scoring (0.5)].

TABLE 1 Clinical and laboratory characteristics of patients at baseline

	ADA	TCZ	*P*-value
Age, mean (range), years	53 (24-78)	56.4 (33-77)	0.516
Sex, female/male, *n*	12/1	18/1	
Duration of symptoms, median (IQR), months	62 (11-147)	142 (72-178)	0.156
ESR, median (IQR), mm/h	48 (34-54)	54 (34-64)	0.389
CRP, median (IQR), mg/dl	0.51 (0.09-0.89)	1.31 (0.24-3.03)	0.089
Swollen joint count, median (IQR)	3 (2-5)	5 (3-7)	0.179
Tender joint count, median (IQR)	5 (1-8)	4 (2-9)	0.984
Patient's global assessment by VAS, median (IQR)	50 (42-65)	67 (40-80)	0.544
Examiner's global assessment by VAS, median (IQR)	40 (40-50)	50 (33-70)	0.56
DAS28-ESR (S.D.)			
Baseline	5.03 (1.16)	5.28 (1.08)	0.575
Week 8	2.96 (0.86)	2.93 (0.81)	0.936
SDAI (S.D.)			
Baseline	21 (10.5)	24.7 (11.3)	0.275
Week 8	7.61 (5.48)	8.84 (4.31)	0.60
TGSS, median (IQR)			
Baseline	99.5 (73-116)	122.75 (98.75-160.75)	0.238
Week 50	108.5 (73-134.5)	125 (99.88-164.88)	0.271

Relationship between positive synovial vascularity and radiographic progression in finger joints

In the ADA group the mean and median of local synovial vascularity at baseline for the MCP and PIP joints were 197 and 0 (range 0-3053) and 218 and 0 (range 0-2414), respectively. In the TCZ group the mean and median of local synovial vascularity at baseline for the MCP and PIP joints were 416 and 0 (range 0-4686) and 167 and 0 (range 0-3195), respectively. Local synovial vascularity in both the ADA and TCZ groups decreased significantly from baseline to week 8 (ADA: MCP $P=0.0001$, PIP $P<0.0001$; TCZ: MCP $P=0.0002$, PIP $P=0.004$). We next categorized finger joints into four groups according to the occurrence of patterns of positive synovial vascularity: joints without synovial vascularity throughout the observational period [the negative (N) group], joints with positive synovial vascularity limited to the period from the baseline to week 8 [the therapeutic response (R) group], joints with intermittent occurrence of positive synovial vascularity in the observational period [the intermittently positive (IP) group] and joints with persistent positive synovial vascularity throughout the observational period [the persistently positive (PP) group]. Each patient had a different pattern of joints with positive synovial vascularity: patients in the N group (ADA $n=2$, TCZ $n=2$), patients in the R group (ADA $n=3$, TCZ $n=3$), patients in the IP or PP groups (ADA $n=3$, TCZ $n=6$) and patients in the mixed R and IP or PP groups (ADA $n=5$, TCZ $n=7$).

The change in the LGSS (ΔLGSS) of the R group showed no progression as compared with the N group or showed improvement of joint damage in the PIP joints of the ADA treatment group (Fig. 1). We next focused on the joints with positive synovial vascularity after week 8, comprising the IP and PP groups. These joints showed an increased ΔLGSS as compared with the N group (Fig. 1). The ΔLGSS between the IP and PP groups showed no significant difference with either ADA or TCZ treatment (Fig. 1).

To analyse the relationship between synovial vascularity and ΔLGSS in more detail in the joints comprising the IP and PP groups, we calculated the sum of synovial vascularity of each finger joint from baseline to week 40 to represent the total exposure to inflammation during the treatment period. The medians of the sum of synovial vascularity with ADA therapy for the MCP and PIP joints were 1456 (range 71-6352) and 1136 (range 71-4757), respectively. The medians of the sum of synovial vascularity with TCZ therapy for the MCP and PIP joints were 2947 (range 71-11289) and 1385 (range 71-5964), respectively. We categorized these joints into two groups: those with a sum of synovial vascularity $\leqslant$ median value [the low-level (L) group], and those with a sum of synovial vascularity $>$ median value [the high-level (H) group]. There were no significant differences in the ΔLGSS between the L group and H group with either ADA or TCZ treatment (Fig. 1).

Intra- and interobserver reliability for power Doppler ultrasonography

Representative PDS images for 20 MCP and 20 PIP joints were randomly chosen, and synovial vascularity was measured three times each by the three ultrasonographers (M.H., F.S. and A.N.). The obtained intraobserver ICC values were 0.997-0.999 for MCP joints and 0.998-0.999 for PIP joints. The interobserver ICC values were 0.992-0.996 for MCP joints and 0.991-0.999 for PIP joints.

Discussion

Our study revealed two noteworthy results. First, this study further emphasized a previous report [7] that early improvement and then disappearance of synovial vascularity resulted in reducing joint damage progression.

FIG. 1 Relationship between positive synovial vascularity and LGSS in finger joints.

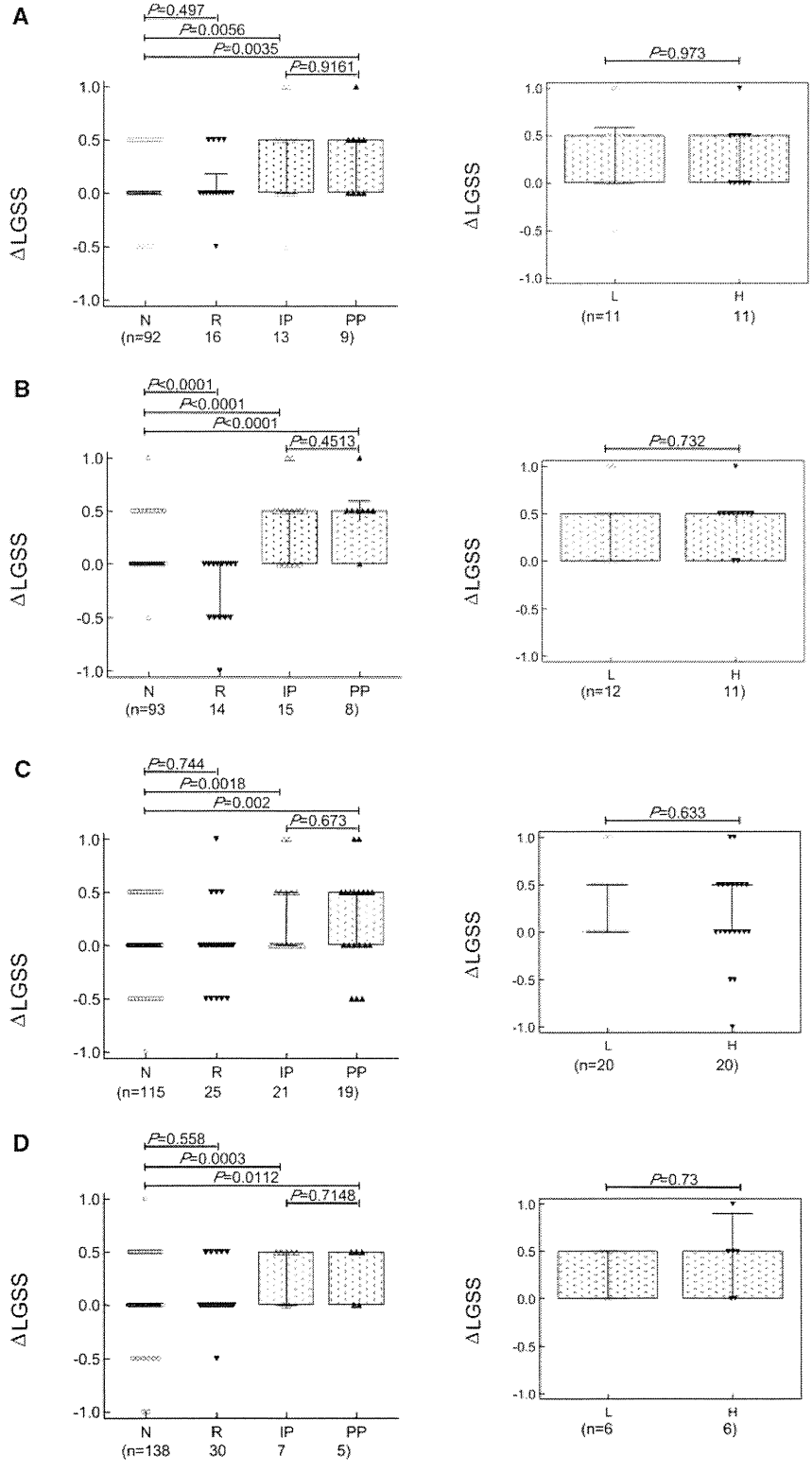

For ADA treatment, ΔLGSS of MCP (**A**) and PIP joints (**B**) is shown. For TCZ treatment, ΔLGSS of MCP (**C**) and PIP joints (**D**) is shown. Graphs on the left side show ΔLGSS of the N, R, IP and PP groups (Results section), which were categorized according to the occasional occurrence of positive synovial vascularity. For each joint in the IP and PP groups, the sum of synovial vascularity from baseline to week 40 was calculated and then categorized as L and H groups (Results section). Graphs on the right side show ΔLGSS of the L and H groups.

Secondly, a novel result was that persistence of positive synovial vascularity in local finger joints showed joint damage progression despite achieving low disease activity by biologic therapies. Interestingly, the ΔLGSS progressed independently of time-integrated joint inflammation estimated by the sum of synovial vascularity or occasional occurrence of positive synovial vascularity. These joints indicate the presence of low-level local joint inflammation, i.e. smouldering inflammation. The smouldering inflammatory joints could be categorized as a variation of subclinical synovitis described below.

Analysis of RA in the clinical remission phase revealed that there were asymptomatic or symptom-limited joints with poor prognosis. This joint inflammation or so-called subclinical synovitis can only be detected with imaging techniques [11–14]. The growing importance of imaging remission of rheumatoid activity has been confirmed, and imaging techniques such as joint ultrasonography have focused on detailed detection of local joint inflammation [15, 16].

Synovial vascularity detected by PDS is irrefutably linked to the level of joint inflammation [17, 18]. Naredo *et al.* [19] reported the correlation between time-integrated values of joint counts for positive synovial vascularity and total joint damage progression at 1 year. From these results, we speculated that increasing and persistent synovial vascularity might result in advanced joint damage progression; hence an increase in the occasional occurrence of positive synovial vascularity or the sum of synovial vascularity worsens the structural damage in smouldering inflammatory joints. Our data revealed that joints with positive synovial vascularity after week 8 (IP and PP groups) showed joint damage progression; however, their ΔLGSS progression did not relate to the occasional occurrence of positive synovial vascularity or the sum of synovial vascularity (Fig. 1). Accordingly, we concluded that the structural damage in joints with smouldering inflammation progressed independently of the level of the sum of synovial vascularity or the occasional occurrence of positive synovial vascularity. Importantly, the result might indicate that even low levels of positive synovial vascularity that occurred only once during the clinical improvement phase showed a risk for structural damage.

Although a correlation between the progression of systemic joint damage and time-integrated values of joint counts for positive synovial vascularity was reported [19], our study, which focused on synovitis and joint damage in individual finger joints, did not show such correlation. Whereas the previous study [19] showed the effect of non-biologic DMARDs, we studied biologic agents that rapidly improved acute inflammation. The DMARDs have slow therapeutic effect; thus the relationship between exposure to inflammation and joint damage progression may be closer in non-biologic DMARD users. Further, our data showed that some patients were in the mixed R and IP or PP group after starting biologic agents. This might indicate a discrepancy between overall therapeutic response and local joint response. Limitations of our study were its small scale and short observation period. Further larger studies are needed to confirm our observations.

In RA, tight control of joint inflammation is necessary for better outcomes. Treatment strategies should be changed according to the clinical response. Monitoring of synovial vascularity has the potential to provide useful joint information for daily practice and to tailor treatment strategies in RA.

Rheumatology key messages

- Finger joints with positive synovial vascularity under low disease activity showed structural deterioration in RA.
- Monitoring of synovial vascularity has the potential to provide useful information for daily practice in RA.

Disclosure statement: The authors have declared no conflicts of interest.

References

1 Jousse-Joulin S, d'Agostino MA, Marhadour T *et al.* Reproducibility of joint swelling assessment by sonography in patients with long-lasting rheumatoid arthritis (SEA-Repro study part II). J Rheumatol 2010;37:938–45.

2 Felson DT, Anderson JJ, Boers M *et al.* Preliminary definition of improvement in rheumatoid arthritis. Arthritis Rheum 1995;38:727–35.

3 Prevoo ML, van 't Hof MA, Kuper HH, van Leeuwen MA, van de Putte LB, van Riel PL. Modified disease activity scores that include twenty-eight-joint counts. Development and validation in a prospective longitudinal study of patients with rheumatoid arthritis. Arthritis Rheum 1995;38:44–8.

4 Koch AE. Review: angiogenesis: implications for rheumatoid arthritis. Arthritis Rheum 1998;41:951–62.

5 Newman JS, Adler RS, Bude RO, Rubin JM. Detection of soft-tissue hyperemia: value of power Doppler sonography. AJR Am J Roentgenol 1994;163:385–9.

6 Naredo E, Moller I, Cruz A, Carmona L, Garrido J. Power Doppler ultrasonographic monitoring of response to anti-tumor necrosis factor therapy in patients with rheumatoid arthritis. Arthritis Rheum 2008;58:2248–56.

7 Fukae J, Isobe M, Kitano A *et al.* Radiographic prognosis of finger joint damage predicted by early alteration in synovial vascularity in patients with rheumatoid arthritis: potential utility of power Doppler sonography in clinical practice. Arthritis Care Res 2011;63:1247–53.

8 Fukae J, Kon Y, Henmi M *et al.* Change of synovial vascularity in a single finger joint assessed by power Doppler sonography correlated with radiographic change in rheumatoid arthritis: comparative study of a novel quantitative score with a semiquantitative score. Arthritis Care Res 2010;62:657–63.

9 Genant HK, Jiang Y, Peterfy C, Lu Y, Redei J, Countryman PJ. Assessment of rheumatoid arthritis using

a modified scoring method on digitized and original radiographs. Arthritis Rheum 1998;41:1583–90.

10 Bruynesteyn K, Boers M, Kostense P, van der Linden S, van der Heijde D. Deciding on progression of joint damage in paired films of individual patients: smallest detectable difference or change. Ann Rheum Dis 2005;64: 179–82.

11 Peluso G, Michelutti A, Bosello S, Gremese E, Tolusso B, Ferraccioli G. Clinical and ultrasonographic remission determines different chances of relapse in early and long standing rheumatoid arthritis. Ann Rheum Dis 2011;70: 172–5.

12 Brown AK, Quinn MA, Karim Z *et al.* Presence of significant synovitis in rheumatoid arthritis patients with disease-modifying antirheumatic drug-induced clinical remission: evidence from an imaging study may explain structural progression. Arthritis Rheum 2006;54: 3761–73.

13 Filippucci E, Iagnocco A, Meenagh G *et al.* Ultrasound imaging for the rheumatologist VII. Ultrasound imaging in rheumatoid arthritis. Clin Exp Rheumatol 2007; 25:5–10.

14 Brown AK, Conaghan PG, Karim Z *et al.* An explanation for the apparent dissociation between clinical remission and continued structural deterioration in rheumatoid arthritis. Arthritis Rheum 2008;58:2958–67.

15 Saleem B, Brown AK, Keen H *et al.* Should imaging be a component of rheumatoid arthritis remission criteria? A comparison between traditional and modified composite remission scores and imaging assessments. Ann Rheum Dis 2011;70:792–8.

16 Dougados M, Devauchelle-Pensec V, Ferlet JF *et al.* The ability of synovitis to predict structural damage in rheumatoid arthritis: a comparative study between clinical examination and ultrasound. Ann Rheum Dis 2012. Advance Access published on 7 June 2012, doi:10.1136/annrheumdis-2012-201469.

17 Schirmer M, Duftner C, Schmidt WA, Dejaco C. Ultrasonography in inflammatory rheumatic disease: an overview. Nat Rev Rheumatol 2011;7:479–88.

18 Lainer-Carr D, Brahn E. Angiogenesis inhibition as a therapeutic approach for inflammatory synovitis. Nat Clin Pract Rheumatol 2007;3:434–42.

19 Naredo E, Collado P, Cruz A *et al.* Longitudinal power Doppler ultrasonographic assessment of joint inflammatory activity in early rheumatoid arthritis: predictive value in disease activity and radiologic progression. Arthritis Rheum 2007;57:116–24.

RHEUMATOLOGY

Rheumatology 2013;52:1775–1784
doi:10.1093/rheumatology/ket234
Advance Access publication 22 July 2013

Original article

Essential role of the p38 mitogen-activated protein kinase pathway in tissue factor gene expression mediated by the phosphatidylserine-dependent antiprothrombin antibody

Kenji Oku[1], Olga Amengual[1], Polona Zigon[2], Tetsuya Horita[1], Shinsuke Yasuda[1] and Tatsuya Atsumi[1]

Abstract

Objective. The aim of this study was to investigate the effects of phosphatidylserine-dependent antiprothrombin antibody (aPS/PT) on the expression of tissue factor (TF) and the signal transduction pathway in procoagulant cells.

Methods. Peripheral blood mononuclear cells (PBMCs) from a healthy donor, murine monocyte RAW264.7 cells and human umbilical vein endothelial cells (HUVECs) were treated with either IgG fractions obtained from APS patients who were positive for aPS/PT or a murine monoclonal aPS/PT antibody, 231D, in the presence of prothrombin. The levels of TF mRNA were measured using real-time PCR. TF function, as measured by procoagulant activity, was determined with a clotting assay. 231D binding on the surface of treated cells was determined by flow cytometric analysis. Screening for phosphorylation of intracellular signalling proteins was conducted using an array assay. Phosphorylation of p38 MAPK was quantitatively analysed with ELISA, and SB203580 was used as a specific inhibitor of p38 MAPK. Specific siRNA for p38 MAPK was used for the knockdown assay.

Results. The IgG fractions from APS patients and 231D induced TF mRNA overexpression and shortening of coagulation time in cells in the presence of prothrombin. The 231D moiety induced phosphorylation of p38 MAPK after binding to the cell surface of RAW264.7 cells. SB203580 or p38 siRNA significantly hampered TF overexpression.

Conclusion. Expression of TF in procoagulant cells was induced by aPS/PT via p38MAPK phosphorylation. This phenomenon may be correlated with the thrombogenicity of APS.

Key words: antiphospholipid syndrome, antiprothrombin antibody, tissue factor, p38 MAPK, procoagulant cell activation.

BASIC

Introduction

APS is a clinical condition characterized by recurrent thrombotic events and/or pregnancy morbidity associated with the persistence of aPLs. aPLs are a large and heterogeneous group of circulating immunoglobulins that appear either idiopathically or in a wide range of infectious or autoimmune diseases [1].

Traditionally aPLs are classified as aCLs, anti-beta-2-glycoprotein I (aβ_2GPI) antibodies or LA. Both aCL and aβ_2GPI are detected by ELISA, and both target the complex of β_2GPI and anionic phospholipids. These antibodies are designated β_2GPI-dependent anticardiolipin antibodies (aCL/β_2GPI) [2]. LA is detected by functional coagulation tests that require a careful and sequential series of examinations, and LA activities are indicative of the existence of heterogeneous antibodies, including aCL/β_2GPI.

[1]Department of Medicine II, Hokkaido University Graduate School of Medicine, Sapporo, Japan and [2]University Medical Centre, Department of Rheumatology, Ljubljana, Slovenia.

Submitted 2 November 2012; revised version accepted 15 May 2013.

Correspondence to: Kenji Oku, Department of Medicine II, Hokkaido University Graduate School of Medicine, N15 W7, Kita-ku, Sapporo 060-8638, Japan. E-mail: kenoku@med.hokudai.ac.jp

Evidence has shown that some LA activities depend on antibodies against prothrombin, which was first proposed as a possible cofactor for LA in 1959 [3]. The pathogenicity of aPT was reported from various institutes [4, 5]. Haj-Yahia *et al.* [6] reported that aPT obtained from mouse immunized with human prothrombin showed pathogenicity in an *ex vivo* model. However, association between antiprothrombin and clinical manifestation of APS is still a subject of controversy [7].

We showed that antibodies against the phosphatidylserine–prothrombin complex (aPS/PT), rather than antibodies against prothrombin alone, are closely associated with APS and LA [8], and their targeted antigen is a complex of anionic phospholipid and its binding protein, an analogue of the cardiolipin–β_2GPI complex. The sensitivity and specificity of aPS/PT for the diagnosis of APS have been assessed in a population with a variety of autoimmune disorders. It is now recognized that aPS/PT may have diagnostic potential, and they have been proposed as a candidate marker of APS and as an alternative test for LA [9–12].

In contrast to the clinical observation of a strong link between aPS/PT and thrombosis, only a few studies have demonstrated the thrombogenicity of aPS/PT. We have established a monoclonal aPS/PT, designated 231D, which specifically binds to phosphatidylserine–prothrombin complex (PS/PT) and possesses strong LA activity [13]. The concentration-dependent LA activity of the monoclonal aPS/PT and the epitope overlap reasonably represent the characteristics of autoimmune aPS/PT.

Tissue factor (TF) is the initiator of the extrinsic coagulation pathway, and we previously reported its upregulation in APS patients [14, 15]. Further, the results of our previous study and those of other studies demonstrated that monoclonal aCL/β_2GPI binds directly to procoagulant cells such as monocytes and endothelial cells (ECs), and that this binding mediates cell dysregulation, which may induce the clinical manifestations of APS [16–19]. When procoagulant cells are exposed to aCL/β_2GPI in the presence of β_2GPI, they produce thrombophilic molecules, particularly TF or adhesion molecules concomitant with activation of the p38 mitogen-activated protein kinase (MAPK) pathway [20–23]. Considering the analogy in the immunological aspects and clinical impact between aCL/β_2GPI and aPS/PT, these two populations of antibodies are likely to share in the pathophysiology of APS.

In this study we investigated the effects of aPS/PT on procoagulant cells by performing *in vitro* assays with purified IgG fractions obtained from the sera of patients with APS who were positive for aPS/PT and negative for aCL/β_2GPI, and with the monoclonal aPS/PT antibody, 231D.

Materials and methods

Monoclonal and autoimmune aPTs

Two murine monoclonal aPTs, 231D and 51A6, were previously established and characterized [13]. Briefly, the monoclonal aPS/PT antibody 231D was established as follows. BALB/c mice were intraperitoneally immunized with human prothrombin emulsified with complete or incomplete Freund's adjuvant. Spleen cells were fused with P3U1 mouse myeloma cells, and cells producing antibodies against PS/PT complex were screened using an aPS/PT ELISA, and the monoclonal antibody was sequentially purified by protein G-Sepharose affinity chromatography. 51A6, the monoclonal antibody directed against prothrombin, was established in the same manner as 231D with the exception of the immunogen used, prethrombin-1, which is a fragment of prothrombin lacking the phospholipid-binding site (Gla domain).

Both monoclonals bind strongly to the PS/PT complex, but not to phosphatidylserine alone; however, 231D has stronger binding to the PS/PT complex than 51A6. 51A6 binds to prothrombin coated on both irradiated and non-irradiated ELISA plates {antiprothrombin-alone (APT-A) activity [24]}; however, 231D shows little binding to prothrombin regardless of the plate type. 231D-spiked plasma has strong LA activity; 51A6-spiked plasma also has LA activity, but it is weaker. Binding of purified IgG from aPS/PT-positive patients with APS to the PS/PT complex is partially inhibited by 231D, but not by 51A6.

Therefore 231D has characteristics common to autoimmune aPS/PT. In contrast, 51A6 binding to prothrombin was not affected by the presence of phosphatidylserine, which is far different from the characteristics of the aPTs found in patients with APS.

IgG fractions were obtained from plasma samples of five APS patients with high titres of IgG aPS/PT in the absence of IgG aCL and aβ_2GPI using protein G-Sepharose affinity chromatography (MAbTrap-TMGII, Pharmacia). The patients included three females with a mean age of 46 (range 36–72) years, disease duration of 3–7 years and one to four past thrombotic events. IgG fractions from patients were pooled as the IgG aPS/PT fraction and frozen until use. Purified IgG fractions from plasma of three healthy individuals were prepared in the same fashion.

The study was performed in accordance with the Declaration of Helsinki and the principles of good clinical practice. Approval was obtained from the local ethics committee (Institutional Review Board of Hokkaido University Hospital), and informed consent was obtained from all subjects.

Cell isolation and preparation

Venous blood was collected from healthy donors into heparinized tubes. Peripheral blood mononuclear cells (PBMCs) were isolated by gradient centrifugation (Ficoll-Paque plus, GE Healthcare, Chalfont St Giles, Buckinghamshire, UK). The cells were then washed with Rosewell Park Memorial Institute (RPMI)-1640 medium (Sigma-Aldrich, St. Louis, MO, USA) supplemented with 10% heat-inactivated fetal calf serum (FCS; GIBCO BRL, Paisley, UK) containing penicillin and streptomycin, followed by centrifugation once at 400 *g* for 5 min at room temperature, and twice for 5 min at 4°C. The cells were then resuspended in RPMI-1640 and counted using the trypan blue dye exclusion method. The murine monocyte

cell line RAW264.7 (American Type Culture Collection number TIB-71) was maintained in an atmosphere of 5% CO_2 at 37°C in DMEM (GIBCO BRL) supplemented with 10% heat-inactivated FCS containing penicillin and streptomycin. Human umbilical vein endothelial cells (HUVECs) (Kurabo, Tokyo, Japan) were maintained under 5% CO_2 at 37°C in HuMedia EB-2 (Kurabo).

Procoagulant cell treatment

Prothrombin, monoclonal aPS/PT (231D) and mouse IgG were added to PBMCs or RAW264.7 cells at a concentration of 10 μg/ml and to HUVECs at a concentration of 15 μg/ml. The IgG aPS/PT fraction (500 μg/ml) or control IgG fraction (500 μg/ml) was added to the cells. Lipopolysaccharide (LPS) was used as positive control at a concentration of 100 ng/ml. The Ca^{2+} concentration in each sample was adjusted to 2.5 mM, which was sufficient to facilitate the binding of prothrombin to phosphatidylserine. The cells were treated for 5 h for TF mRNA determination, for 15 min for p38 MAPK phosphorylation and for 12 h for clotting assay.

Flow cytometry assay with IIF staining

To observe the binding of monoclonal antibody to the cell surface, a flow cytometry assay with IIF staining was performed. Mouse monoclonal antibodies and control IgG were added to RAW264.7 with or without prothrombin. Cells were washed and collected after 4 h of incubation. Diluted FITC-conjugated AffiniPure donkey anti-mouse IgG antibody (Sigma-Aldrich Co.) was added to the cell suspension and then analysed with a flow cytometry (FACS) analyser.

RNA isolation and quantitative TaqMan real-time PCR

Total RNA was isolated from the cells using TRIzol reagent (Invitrogen, Carlsbad, CA, USA) and an RNeasy Mini kit (Qiagen GmbH, Hilden, Germany) and stored at −80°C until use.

Complementary DNA (cDNA) was generated using the SuperScript II first-strand cDNA pre-amplification system (Gibco BRL, Rockville, MD, USA) according to the random primer protocol provided by the manufacturer. The induction of mRNA was measured by real-time PCR using TaqMan Universal PCR Master Mix and gene-specific sets of Assay-on-Demand Gene Expression probes (Applied Biosystems, Foster City, CA, USA) with the ABI PRISM 7000 Sequence Detection System (Applied Biosystems).

Messenger RNA samples were analysed in at least three similar real-time PCR procedures. Negative controls containing water instead of RNA were simultaneously run to rule out cross-contamination. Relative expression was quantified by the ΔΔCt method and normalized to GAPDH.

Clotting assay

To evaluate the procoagulant activity of cells, the clotting time of PBMCs was measured using an automated STA-R coagulation analyzer (Diagnostica Stago, Asnière, France). After three washes in Tris-buffered saline (TBS) containing 0.05% Tween 20 (Sigma-Aldrich Co.) and 5 mM $CaCl_2$ (TBS-Tween-Ca), 2 ml of normal human plasma was added to 2 ml of cell fluid (1×10^6 cells/ml). The reduction in the clotting time compared with the normal control sample was interpreted as increased coagulation function and was attributed to the expression of TF.

Detection of intracellular signal protein phosphorylation

For parallel determination of the relative phosphorylation levels of intracellular signal proteins, particularly MAPKs and other serine/threonine kinases, an array assay was performed using the Human Proteome Profiler Array kit (R&D Systems, Minneapolis, MN, USA) following the standard procedure provided by the manufacturer. Briefly, concentrated PBMC lysates obtained from normal healthy controls were adjusted according to the manufacturer's instructions following exposure to the stimulators [231D (10 μg/ml) with and without prothrombin (10 μg/ml)] for 15 min. The lysates were added to the array and exposed to X-rays for 5 min.

Quantitative analysis of serine-threonine kinase phosphorylation by cellular activation ELISA

Quantitative analysis of intracellular signal phosphorylation in RAW264.7 mouse monocytes was performed using a Cellular Activation of Signaling ELISA (CASE) kit (SABiosciences Corporation, Frederick, MD, USA) following the standard method provided by the manufacturer. The phosphorylation of p38 MAPK, c-Jun N-terminal kinase (JNK), extracellular regulated kinase (ERK1/2) and Akt (protein kinase B) was carried out as follows. Briefly, experimentally treated cells were seeded in 96-well plates and fixed with paraformaldehyde. Two primary antibodies, one that recognizes phosphorylated serine-threonine kinases and another that recognizes serine-threonine kinases regardless of phosphorylation were used to detect the relative amount of phosphorylated serine-threonine kinases, which was assayed by measuring the optical density (OD) on an ELISA plate reader. The OD was measured at 450 nm and normalized to the cell number (OD_{540}). Then the OD ratio (OD_{450}:OD_{540}) of phospho-serine-threonine kinase-specific antibody (OD phospho-kinases) was normalized to the pan-serine-threonine kinase-specific antibody OD ratio (OD pan-kinases) under the same experimental conditions, indicating the relative extent of serine-threonine kinase phosphorylation (OD phospho-kinases/OD pan-kinases). Finally, to determine the relative extent of target protein phosphorylation, the OD phospho-kinases/OD pan-kinases ratio of each sample was compared with unstimulated samples to calculate the relative amount of serine-threonine kinase phosphorylation.

RNA interference

RNA interference was carried out with Accell small interfering RNA (siRNA; Dharmacon, Lafayette, CO, USA), predesigned pools of four oligonucleotides, using the Accell siRNA delivery protocol following the manufacturer's

instructions. Briefly, 8 h after plating, PBMC from healthy controls (5×10^5 cells/well) were transfected with 1 μM p38 MAPK-α (MAPK 14) Accell siRNA or Accell non-targeting siRNA in 100 μl Accell siRNA delivery media (Dharmacon). Cells were incubated at 37°C 72 h before assessment of RNAi knockdown effect.

Proteins

Fatty acid-free BSA was obtained from Sigma-Aldrich. LPS was removed from the antibody preparation by using DetoxiGel (Pierce, Rockford, IL, USA), and its absence was confirmed using the Limulus amebocyte lysate assay (Limulus ES-II Single Test Wako; Wako, Osaka, Japan). Human prothrombin was obtained from Enzyme Research (South Bend, IN, USA).

Statistical analysis

Means of the various treated and control groups were compared by Student's unpaired *t*-test. SPSS II for Windows (SPSS Japan Inc., Tokyo, Japan) was used for all calculations.

Results

Upregulation of TF mRNA expression in PBMCs and RAW264.7 cells treated with IgG from APS patients' plasma and monoclonal aPS/PT

Immunoglobulin G isolated from APS patients' plasma and LPS significantly increased the expression of TF mRNA in PBMCs. In contrast, IgG from healthy controls did not increase the expression of TF mRNA in PBMCs (Fig. 1A).

231D in the presence of prothrombin significantly increased the expression of TF mRNA in PBMCs and in RAW264.7 cells. However, 231D in the absence of prothrombin or control IgG with prothrombin did not increase TF mRNA expression (Fig. 1B and C).

Procoagulant activity of PBMCs treated with aPS/PT

TF function in aPS/PT-treated cells, measured by procoagulant activity, was analysed using a clotting assay. The clotting time of the cell fluid from PBMCs treated with IgG isolated from APS patients' plasma in the presence of prothrombin was significantly reduced. In contrast, the coagulation time of cell fluid treated with APS patients' IgG alone or IgG from healthy controls with prothrombin was not reduced (Fig. 2A). In addition, the clotting time of the cell fluid from PBMCs treated with 231D in the presence of prothrombin was significantly reduced. The coagulation time of cell fluid treated with 231D alone or with control IgG and prothrombin was not reduced (Fig. 2B).

Monoclonal aPS/PT binding to the cell surface of RAW264.7 cells was detected by a flow cytometric assay with IIF staining

RAW264.7 were treated with monoclonal aPTs (51A6 and 231D) or control mouse IgG at 37°C under 5% CO_2 for 4 h. In the presence of prothrombin, 75.9% of 231D-treated cells bound to antibody, while only 41.4% of 51A6-treated cells and 0.5% of control IgG-treated cells bound to antibody. In the absence of prothrombin, cells treated with antibodies showed almost no binding to the 231D, 51A6 and control IgG antibodies (3.8%, 0.1% and 0.3%, respectively) (Fig. 3).

Intracellular signal protein phosphorylation in PBMCs treated with monoclonal aPS/PT

Results of the array assay showed phosphorylation of p38 (p38α) in PBMCs treated with 231D in the presence of prothrombin. However, no p38 phosphorylation was detected in cells treated with 231D in the absence of prothrombin. Phosphorylation of other serine/threonine kinases or other MAPK family proteins was also not detected, therefore p38 was presumed to be the major signal protein involved in monocyte activation by aPS/PT.

Quantitative analysis of intracellular signal phosphorylation in RAW264.7 cells treated with monoclonal aPS/PT

Based on the results of the array assay, serine-threonine kinases including p38 phosphorylation was quantitatively analysed using an ELISA CASE kit. In the presence of prothrombin, 231D significantly increased the relative amount of p38 phosphorylation compared with the untreated control up to 1.7-fold. There was no increase in the amount of relative p38 phosphorylation with 231D in the absence of prothrombin, or with control mouse IgG plus prothrombin (Fig. 4A). The relative amount of phosphorylation in other serine-threonine kinases such as JNK, ERK1/2 and Akt were not detected (Fig. 4B–D).

Effect of p38 MAPK inhibitor on PBMCs TF expression induced by monoclonal aPS/PT treatment

To elucidate the role of p38 MAPK in TF mRNA expression, we investigated the effect of a p38 MAPK inhibitor on cells treated with monoclonal aPS/PT. The p38-specific inhibitor SB203580 significantly reduced TF mRNA overexpression in 231D-treated PBMCs (Fig. 5A) and RAW264.7 cells compared with the untreated control (Fig. 5B). However, its inactive analogue SB202474 did not affect TF mRNA expression. Addition of SB203580 to 231D-treated cells decreased TF mRNA expression 80–90%.

Effect of siRNA reagents on PBMC TF expression induced by monoclonal aPS/PT treatment

The effect of p38 siRNA on PBMC TF mRNA expression induced by 231D treatment was investigated as indicated. The expression of TF mRNA on 231D-treated PBMCs was significantly offset by pre-treatment of p38 siRNA. In contrast, pre-treatment of control siRNA did not affect TF mRNA expression on 231D-treated PBMCs (Fig. 6).

Upregulation of TF mRNA expression and adhesion molecules in HUVECs induced by monoclonal aPS/PT

The expression of TF mRNA was significantly upregulated in HUVECs treated with 231D in the presence of

FIG. 1 Upregulation of TF mRNA expression by aPS/PT.

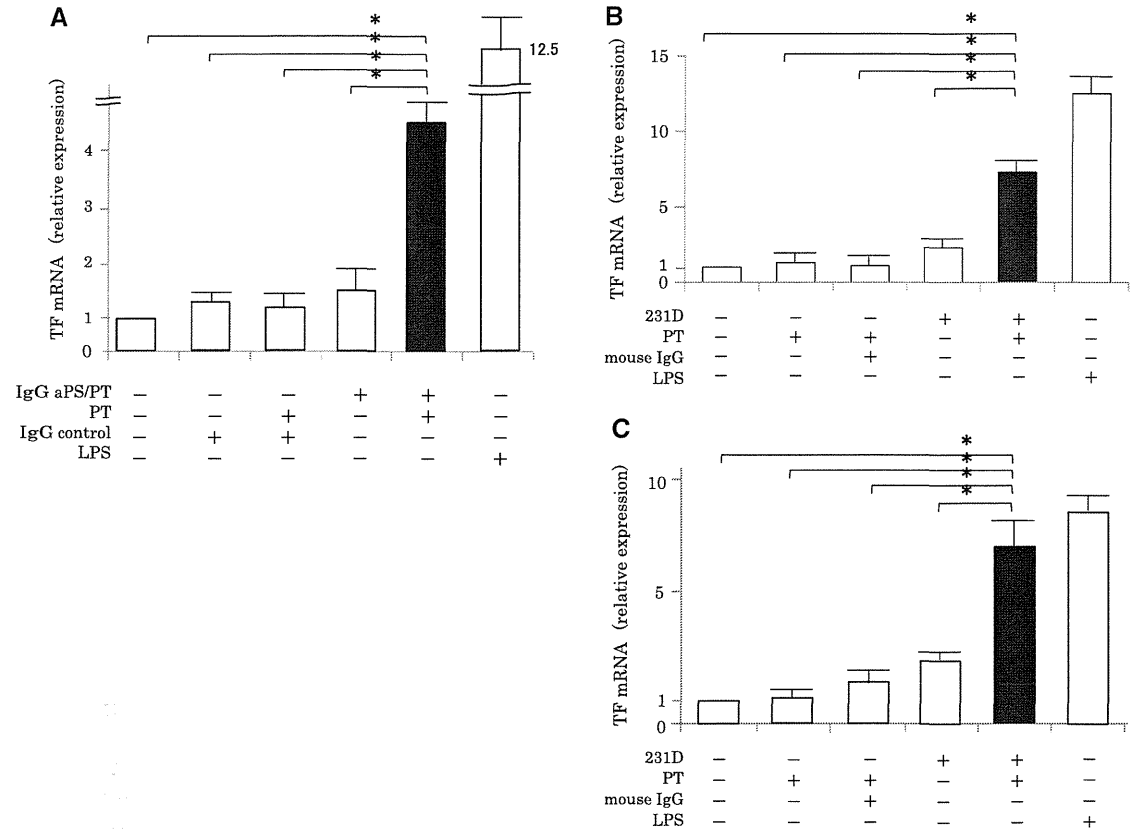

RAW264.7 cells or PBMCs obtained from normal healthy controls were exposed to the substances described below for 5 h. IgG extracted from APS patients positive for aPS/PT (IgG aPS/PT) or IgG extracted from healthy controls (IgG control) was added at 500 μg/ml. Prothrombin (PT), 231D and mouse control IgG (mouse IgG) were added at a concentration of 10 μg/ml and LPS was added at a concentration of 100 mg/ml. *$P < 0.005$. Vertical axes represent the relative expression levels of TF mRNA determined by real-time PCR. The bars represent the mean ± S.E. of three independent experiments. (**A**) The relative TF mRNA expression levels in PBMCs treated with an IgG fraction from aPS/PT-positive patients or an IgG fraction from healthy controls. (**B**) Relative TF mRNA expression levels in PBMCs treated with 231D or mouse control IgG. (**C**) The relative TF mRNA expression levels in RAW264.7 cells treated with 231D or mouse control IgG were measured.

prothrombin (PT + 231D *vs* baseline, 231D alone and PT + control IgG: 2.5 ± 0.7 *vs* 1, 1.2 ± 0.3 and 1.31 ± 0.24; all, $P < 0.005$). The p38-specific inhibitor SB203580 significantly reduced TF mRNA overexpression in 231D-treated HUVECs [SB203580 (+) *vs* SB203580 (−): 1.4 ± 0.2 *vs* 2.5 ± 0.7; $P < 0.005$]; however, its inactive analogue SB202474 did not affect TF mRNA overexpression.

The expression levels of vascular cell adhesion molecule-1 (VCAM-1), platelet-endothelial cell adhesion molecule-1 (PCAM-1) and endothelin-1 mRNA were significantly upregulated 2- to 3-fold in HUVECs treated with 231D in the presence of prothrombin. However, in the absence of prothrombin, 231D did not affect the expression of these adhesion molecules (PT + 231D *vs* baseline, 231D alone and PT + control IgG; VCAM-1: 2.1 ± 0.6 *vs* 1, 1.4 ± 0.1 and 1.1 ± 0.2, PCAM-1: 2.8 ± 0.3 *vs* 1, 1.3 ± 0.0 and 1.8 ± 0.3, selectin: 2.0 ± 0.4 *vs* 1, 1.3 ± 0.2 and 1.1 ± 0.4; all, $P < 0.01$).

Discussion

In this study we showed that IgG fractions and monoclonal aPS/PT induced TF in procoagulant cells. Monoclonal aPS/PT bound to monocytes using prothrombin as a cofactor for binding. Further, we demonstrated that treatment by aPS/PT induces the phosphorylation of p38 MAPK in these procoagulant cells. The coagulation process *in vivo* is complicated and various cells or molecules other than monocytes or endothelial cells are involved. Obviously there are certain limitations in discussing aPS/PT-induced thrombosis from the current results. However, our results showed that TF, the key protein in the coagulation pathway, is overproduced by its main sources in the circulation, monocytes and endothelial cells. Upregulation of blood-borne TF indicates increased procoagulant activity that is considered one of the most important characteristics of aPL-induced thrombosis.

Fig. 2 Procoagulant activity of cells treated with aPS/PT.

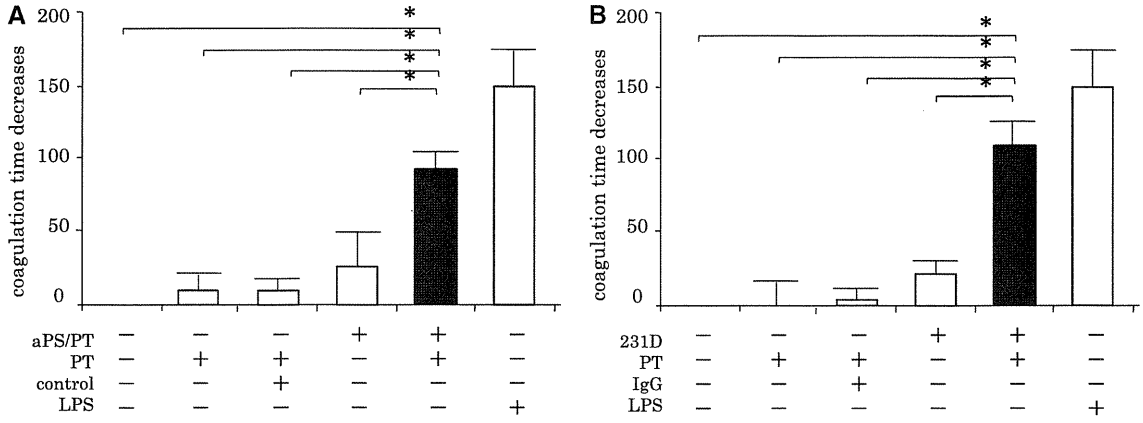

PBMCs obtained from normal healthy donors were exposed to the substances described below for 5 h. The cells were washed and then added to normal healthy plasma, and coagulation time was measured. The reduction in coagulation time was calculated by subtracting the coagulation time of each treated sample from that of unstimulated cells. The bars represent the mean ± S.E. of three independent experiments. *$P < 0.005$. (**A**) PBMCs treated with IgG fractions from patients positive for aPS/PT (aPS/PT) or IgG fraction from healthy controls (control) (500 μg/ml) in the presence or absence of prothrombin (PT). (**B**) PBMCs treated with 231D or mouse control IgG (IgG) (10 μg/ml).

Fig. 3 Binding of aPS/PT to the surface of RAW264.7 cells.

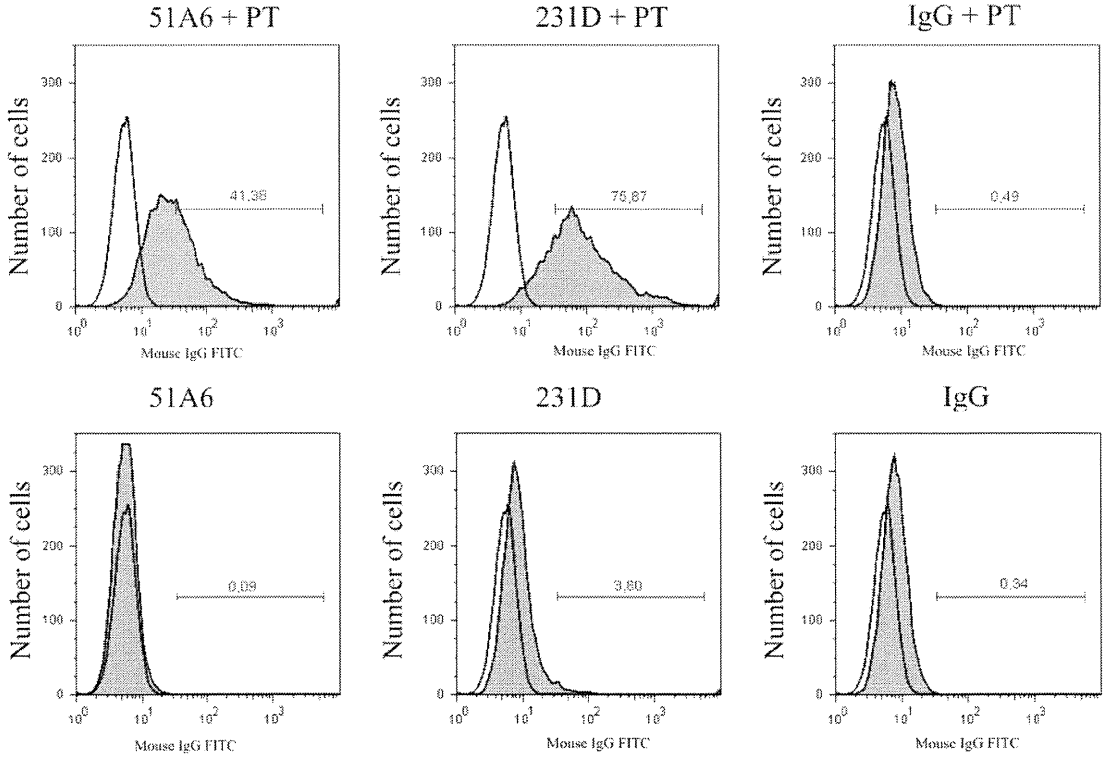

Murine monoclonal anti-prothrombin antibodies (51A6, 231D) and control murine IgG (IgG) were added to RAW264.7 cells at a concentration of 7.5 μg/ml with or without prothrombin (PT) (10 μg/ml), and then incubated for 4 h. After incubation, FITC-conjugated anti-mouse IgG antibody was added to the cell suspension and then analysed with a FACS analyzer. The vertical axes represent the number of cells and the horizontal axes represent the FITC fluorescence intensity.

FIG. 4 Quantitative analysis of serine-threonine kinase phosphorylation in aPS/PT-treated cells.

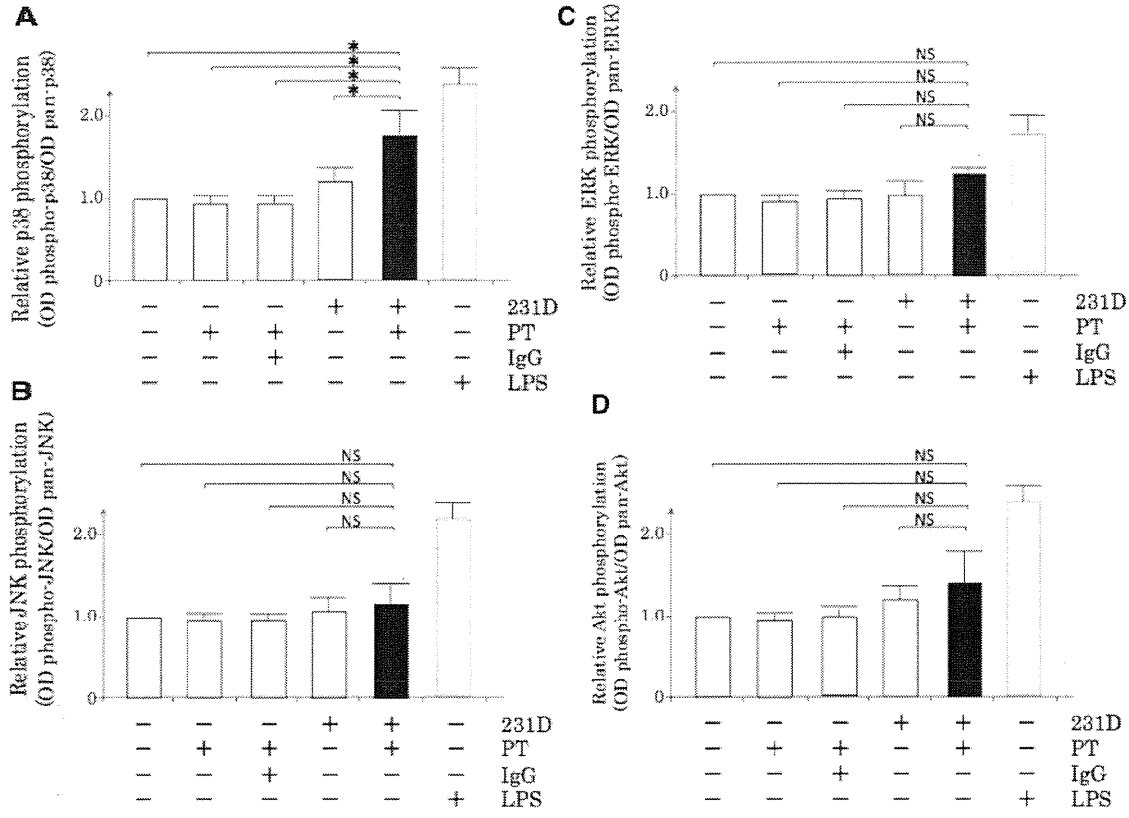

RAW264.7 cells were exposed to the substances described below for 15 min. Prothrombin (PT), 231D and mouse control IgG (IgG) were added at a concentration of 10 μg/ml and LPS was added at a concentration of 100 ng/ml. The relative OD ratio of each sample was measured and calculated as described in the Materials and methods section. *$P < 0.005$, NS: not statistically significant.

FIG. 5 p38 MAPK inhibition assay in aPS/PT-treated cells.

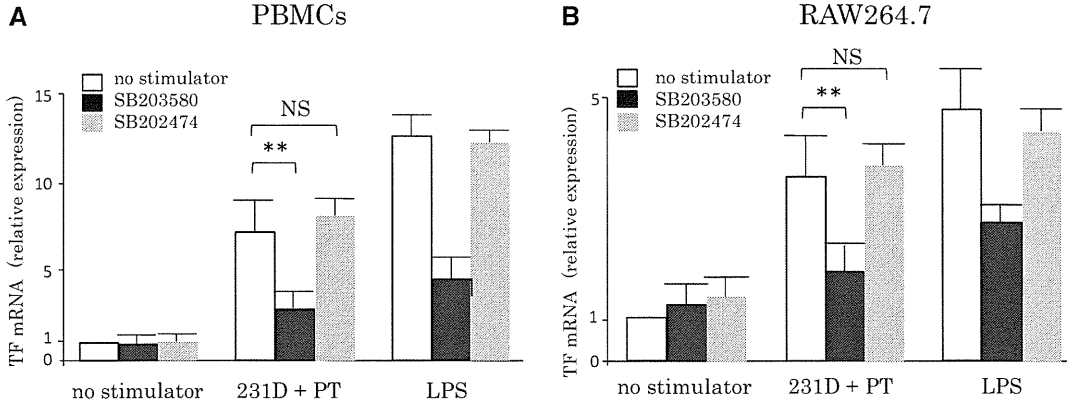

PBMCs and the mouse monocyte cell line, RAW264.7, were exposed to stimulators for 5 h. Prothrombin (PT) and 231D were added at a concentration of 10 μg/ml and LPS was added at 100 ng/ml. Cells were pretreated with the p38-specific inhibitor SB203580 (1 μM) or its inactive analogue SB202474 (1 μM) for 30 min followed by treatment with stimulators. Vertical axes represent the relative expression levels of TF mRNA detected by real-time PCR. The bars represent the mean ± S.E. of three independent experiments. **$P < 0.001$, NS: not statistically significant. (**A**) The relative TF mRNA expression levels in PBMCs. (**B**) The relative TF mRNA expression levels in RAW264.7 cells.

FIG. 6 RNA interference of p38 MAPK in aPS/PT-treated cells.

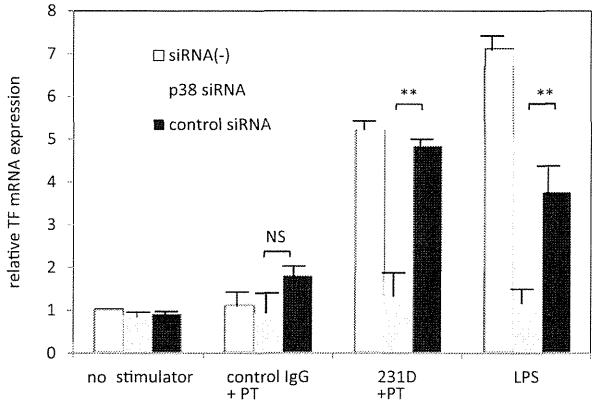

PBMCs were pretreated for 72 h with siRNA of p38 MAPK or the control and subsequently exposed to stimulators for 5 h. Prothrombin (PT) and 231D were added at a concentration of 10 μg/ml and LPS was added at 100 ng/ml. The vertical axis represents the relative expression level of TF mRNA detected by real-time PCR. The bars represent the mean ± S.E. of three independent experiments. $^{**}P < 0.001$, NS: not statistically significant.

231D and 51A6 significantly bound to the membranes of monocytes in the presence of prothrombin. The binding of 231D to the cell surface was clearly stronger than that of 51A6. This observation was similar to our previous report that 231D had stronger binding to the PS/PT complex than 51A6 [13], suggesting that the monoclonal antibodies bind to prothrombin complexed with phosphatidylserine on the cell surface.

Our data suggest that TF production induced by aPS/PT in procoagulant cells is mainly induced via activation of the p38 MAPK pathway, which is similar to past reports showing that p38 MAPK was the main pathway of aCL/β_2GPI-induced cell activation. It is interesting that antibodies recognizing different proteins seem at least partially to utilize a common signalling pathway. Our findings are in agreement with the clinical observation that the manifestations of APS do not differ in patients with different antibody profiles.

Protein kinases are key regulators of cellular signalling, inflammation, cell differentiation and cell death. Thus they have been attractive targets for the treatment of neoplasms and inflammatory diseases [25–27].

p38 MAPK belongs to the MAPK signal protein family and is strongly activated by environmental stress or inflammatory cytokines such as TNF-α, IL-1β and IL-18 [28–30]. Consequently p38 MAPK activation is considered critical for physiological immune responses, and p38 MAPK dysfunction is related to the pathology of autoimmune diseases other than APS [31–33].

In the present study, phosphorylation of signal proteins, such as those in the MAPK protein family and serine/threonine kinases, was screened in aPS/PT-treated cells using a proteome array and major signals were quantitatively measured by ELISA tests. No proteins other than p38 MAPK were found to be phosphorylated. Further, specific p38 MAPK inhibitors or knockdown of p38 MAPK mRNA effectively inhibited procoagulant cell activation. Therefore p38 MAPK is suggested as a major signal protein for the activation of aPS/PT-induced procoagulant cells. Although a previous study showed that ERK activation was observed in cells treated with IgG fractions from APS patients [22], an ERK inhibitor did not abolish TF expression in procoagulant cells, suggesting that ERK does not play a major role in cell activation. We also did not detect the ERK phosphorylation in our aPS/PT-treated cells.

The two major aPLs, aCL/β_2GPI and aPS/PT, are suggested to activate procoagulant cells primarily through p38 MAPK phosphorylation, therefore inhibition of p38 MAPK appears to be a promising modality for the treatment of APS. Since p38 MAPK contributes to various cell activities, its non-specific inhibition might result in severe complications. In fact, clinical trials of p38 inhibitors for a variety of diseases have been carried out; however, most of the trials encountered several complications and were unsuccessful [34]. A more realistic and practical strategy would be to target a more specific molecule involved in the activation of aPL-induced procoagulant cells.

Some reports have demonstrated possible receptors for aCL/β_2GPI-induced cell activation on procoagulant cells. Annexin A2 is a receptor for tissue plasminogen activator and plasminogen that is found on the surface of ECs and monocytes, and on the brush-border membrane of placental syncytiotrophoblasts, all of which are recognized targets of pathogenic aPLs [35, 36]. Annexin A2 interacts with the β_2GPI-aCL/β_2GPI complex on EC and monocyte surfaces, mediating cell activation [37–39]. The involvement of annexin A2 in aPL-mediated pathogenic effects has been reported *in vitro* and *in vivo* [40, 41]. However, it is still not clear whether such a receptor is actually involved in cell activation because annexin A2 is not a transmembrane protein. Further, it has been proposed that activation of the signalling responses required another transmembrane adaptor protein(s) that associates with annexin A2 on the EC surface [42].

The Toll-like receptor (TLR) family, in particular, TLR-2 and TLR-4 [43–45], may also play a role in the interaction of the β_2GPI-aCL/β_2GPI complex [42]. Adhered β_2GPI interacts with TLR-4 and aCL/β_2GPI cross-links β_2GPI and the TLR-4 complex, eventually triggering the signalling cascade activation. Moreover, TLR-4 is the putative adaptor protein for annexin A2 [38].

Further investigations have shown that megalin/gp330 [46] and apolipoprotein E receptor 2′ [47–49] are putative receptors for aCL/β_2GPI. Recently we identified the gelsolin/integrin α5β1 complex as a novel receptor of aCL/β_2GPI [50].

In contrast to the intensive investigation of aCL/β_2GPI thrombogenicity, no data are available on the mechanism of aPS/PT-dependent procoagulant cell activation. It is not yet known if aCL/β_2GPI and aPS/PT have a common

cell surface receptor and upstream signals of p38 MAPK. However, we believe that our data are the first to show the critical pathway of the procoagulant state related to antibodies against prothrombin.

There are several reports showing the correlation between aPS/PT and APS-related pregnancy morbidity [51–53] that are subject to further investigation to clarify the molecular mechanism of the manifestation. Identification and comparison of the receptors for aPS/PT and aCL/β_2GPI will help elucidate the pathogenicity of aPLs and the mechanisms of APS pathology.

Rheumatology key messages

- Phosphatidylserine-dependent aPT induced TF expressions on procoagulant cells *in vitro*.
- Similar to aCL, phosphatidylserine-dependent aPT induced cell activation via the p38 MAPK pathway.
- Cell activation via the p38 MAPK pathway may partially explain the pathogenesis of APS thrombosis.

Funding: This work was supported by the Japanese Ministry of Health, Labour and Welfare, the Japanese Ministry of Education, Culture, Sports, Science and Technology (MTX) and the Japanese Society for the Promotion of the Science (JSPS).

Disclosure statement: The authors have declared no conflicts of interest.

References

1 Atsumi T, Amengual O, Koike T. Antiphospholipid syndrome: pathogenesis. In: Lahita R, ed. Systemic lupus erythematosus, 5th edn. San Diego, CA: Academic Press, 2010:945–66.

2 Hashimoto Y, Kawamura M, Ichikawa K *et al*. Anticardiolipin antibodies in NZW x BXSB F1 mice. A model of antiphospholipid syndrome. J Immunol 1992; 149:1063–8.

3 Loeliger A. Prothrombin as a co-factor of the circulating anticoagulant in systemic lupus erythematosus? Thromb Diath Haemorrh 1959;3:237–56.

4 von Landenberg P, Matthias T, Zaech J *et al*. Antiprothrombin antibodies are associated with pregnancy loss in patients with the antiphospholipid syndrome. Am J Reprod Immunol 2003;49:51–6.

5 Zhao Y, Rumold R, Zhu M *et al*. An IgG antiprothrombin antibody enhances prothrombin binding to damaged endothelial cells and shortens plasma coagulation times. Arthritis Rheum 1999;42:2132–8.

6 Haj-Yahia S, Sherer Y, Blank M *et al*. Anti-prothrombin antibodies cause thrombosis in a novel qualitative ex-vivo animal model. Lupus 2003;12:364–9.

7 Galli M. Should we include anti-prothrombin antibodies in the screening for the antiphospholipid syndrome? J Autoimmun 2000;15:101–5.

8 Atsumi T, Ieko M, Bertolaccini ML *et al*. Association of autoantibodies against the phosphatidylserine-prothrombin complex with manifestations of the antiphospholipid syndrome and with the presence of lupus anticoagulant. Arthritis Rheum 2000;43:1982–93.

9 Oku K, Atsumi T, Amengual O *et al*. Antiprothrombin antibody testing: detection and clinical utility. Semin Thromb Hemost 2008;34:335–9.

10 Hoxha A, Ruffatti A, Tonello M *et al*. Antiphosphatidylserine/prothrombin antibodies in primary antiphospholipid syndrome. Lupus 2012;21:787–9.

11 Zigon P, Cucnik S, Ambrozic A *et al*. Antibodies to phosphatidylserine/prothrombin complex as an additional diagnostic marker of APS? Lupus 2012;21:790–2.

12 Otomo K, Atsumi T, Amengual O *et al*. Efficacy of the antiphospholipid score for the diagnosis of antiphospholipid syndrome and its predictive value for thrombotic events. Arthritis Rheum 2012;64:504–12.

13 Sakai Y, Atsumi T, Ieko M *et al*. The effects of phosphatidylserine-dependent antiprothrombin antibody on thrombin generation. Arthritis Rheum 2009;60:2457–67.

14 Atsumi T, Khamashta MA, Amengual O *et al*. Up-regulated tissue factor expression in antiphospholipid syndrome. Thromb Haemost 1997;77:222–3.

15 Amengual O, Atsumi T, Khamashta MA *et al*. The role of the tissue factor pathway in the hypercoagulable state in patients with the antiphospholipid syndrome. Thromb Haemost 1998;79:276–81.

16 Xu G, Wen H, Zhou H *et al*. Involvement of IRAKs and TRAFs in anti-beta(2)GPI/beta(2)GPI-induced tissue factor expression in THP-1 cells. Thromb Haemost 2011;106: 1158–69.

17 Meroni PL, Raschi E, Testoni C *et al*. Endothelial cell activation by antiphospholipid antibodies. Clin Immunol 2004;112:169–74.

18 Reverter JC, Tassies D, Font J *et al*. Effects of human monoclonal anticardiolipin antibodies on platelet function and on tissue factor expression on monocytes. Arthritis Rheum 1998;41:1420–7.

19 Pierangeli SS, Colden-Stanfield M, Liu X *et al*. Antiphospholipid antibodies from antiphospholipid syndrome patients activate endothelial cells in vitro and in vivo. Circulation 1999;99:1997–2002.

20 Bohgaki M, Atsumi T, Yamashita Y *et al*. The p38 mitogen-activated protein kinase (MAPK) pathway mediates induction of the tissue factor gene in monocytes stimulated with human monoclonal anti-beta2Glycoprotein I antibodies. Int Immunol 2004;16:1633–41.

21 Vega-Ostertag M, Casper K, Swerlick R *et al*. Involvement of p38 MAPK in the up-regulation of tissue factor on endothelial cells by antiphospholipid antibodies. Arthritis Rheum 2005;52:1545–54.

22 Lopez-Pedrera C, Buendia P, Cuadrado MJ *et al*. Antiphospholipid antibodies from patients with the antiphospholipid syndrome induce monocyte tissue factor expression through the simultaneous activation of NF-kappaB/Rel proteins via the p38 mitogen-activated protein kinase pathway, and of the MEK-1/ERK pathway. Arthritis Rheum 2006;54:301–11.

23 Zhou H, Wolberg AS, Roubey RA. Characterization of monocyte tissue factor activity induced by IgG antiphospholipid antibodies and inhibition by dilazep. Blood 2004; 104:2353–8.

24 Amengual O, Atsumi T, Koike T. Specificities, properties, and clinical significance of antiprothrombin antibodies. Arthritis Rheum 2003;48:886–95.

25 Ivison SM, Graham NR, Bernales CQ *et al.* Protein kinase D interaction with TLR5 is required for inflammatory signaling in response to bacterial flagellin. J Immunol 2007; 178:5735–43.

26 Zhao X, Shi C, Wang X *et al.* Protein kinase C modulates the pulmonary inflammatory response in acute pancreatitis. Respir Physiol Neurobiol 2006;152:16–26.

27 Guma M, Hammaker D, Topolewski K *et al.* Pro- and anti-inflammatory functions of the p38 pathway in rheumatoid arthritis: Advantages of targeting upstream kinases MKK3 or MKK6. Arthritis Rheum 2013 (in press).

28 Seo YJ, Pritzl CJ, Vijayan M *et al.* Sphingosine analogue AAL-R increases TLR7-mediated dendritic cell responses via p38 and type I IFN signaling pathways. J Immunol 2012;188:4759–68.

29 Mavropoulos A, Sully G, Cope AP *et al.* Stabilization of IFN-gamma mRNA by MAPK p38 in IL-12- and IL-18-stimulated human NK cells. Blood 2005;105:282–8.

30 O'Sullivan AW, Wang JH, Redmond HP. The role of P38 MAPK and PKC in BLP induced TNF-alpha release, apoptosis, and NFkappaB activation in THP-1 monocyte cells. J Surg Res 2009;151:138–44.

31 Noubade R, Krementsov DN, Del Rio R *et al.* Activation of p38 MAPK in CD4 T cells controls IL-17 production and autoimmune encephalomyelitis. Blood 2011;118: 3290–300.

32 Moon C, Ahn M, Kim H *et al.* Activation of p38 mitogen-activated protein kinase in the early and peak phases of autoimmune neuritis in rat sciatic nerves. Brain Res 2005; 1040:208–13.

33 Berkowitz P, Chua M, Liu Z *et al.* Autoantibodies in the autoimmune disease pemphigus foliaceus induce blistering via p38 mitogen-activated protein kinase-dependent signaling in the skin. Am J Pathol 2008;173:1628–36.

34 Schreiber S, Feagan B, D'Haens G *et al.* Oral p38 mitogen-activated protein kinase inhibition with BIRB 796 for active Crohn's disease: a randomized, double-blind, placebo-controlled trial. Clin Gastroenterol Hepatol 2006;4: 325–34.

35 Hajjar KA, Jacovina AT, Chacko J. An endothelial cell receptor for plasminogen/tissue plasminogen activator. I. Identity with annexin II. J Biol Chem 1994;269:21191–7.

36 Kaczan-Bourgois D, Salles JP, Hullin F *et al.* Increased content of annexin II (p36) and p11 in human placenta brush-border membrane vesicles during syncytiotrophoblast maturation and differentiation. Placenta 1996;17: 669–76.

37 Ma K, Simantov R, Zhang JC *et al.* High affinity binding of beta 2-glycoprotein I to human endothelial cells is mediated by annexin II. J Biol Chem 2000;275:15541–8.

38 Zhang J, McCrae KR. Annexin A2 mediates endothelial cell activation by antiphospholipid/anti-beta2 glycoprotein I antibodies. Blood 2005;105:1964–9.

39 Zhou H, Ling S, Yu Y *et al.* Involvement of annexin A2 in anti-beta2GPI/beta2GPI-induced tissue factor expression on monocytes. Cell Res 2007;17:737–9.

40 Zhou H, Yan Y, Xu G *et al.* Toll-like receptor (TLR)-4 mediates anti-beta2GPI/beta2GPI-induced tissue factor expression in THP-1 cells. Clin Exp Immunol 2011;163: 189–98.

41 Romay-Penabad Z, Montiel-Manzano MG, Shilagard T *et al.* Annexin A2 is involved in antiphospholipid antibody-mediated pathogenic effects in vitro and in vivo. Blood 2009;114:3074–83.

42 Raschi E, Testoni C, Bosisio D *et al.* Role of the MyD88 transduction signaling pathway in endothelial activation by antiphospholipid antibodies. Blood 2003; 101:3495–500.

43 Pierangeli SS, Vega-Ostertag ME, Raschi E *et al.* Toll-like receptor and antiphospholipid mediated thrombosis: in vivo studies. Ann Rheum Dis 2007;66:1327–33.

44 Satta N, Dunoyer-Geindre S, Reber G *et al.* The role of TLR2 in the inflammatory activation of mouse fibroblasts by human antiphospholipid antibodies. Blood 2007;109: 1507–14.

45 Sorice M, Longo A, Capozzi A *et al.* Anti-beta2-glycoprotein I antibodies induce monocyte release of tumor necrosis factor alpha and tissue factor by signal transduction pathways involving lipid rafts. Arthritis Rheum 2007;56: 2687–97.

46 Pennings MT, van Lummel M, Derksen RH *et al.* Interaction of beta2-glycoprotein I with members of the low density lipoprotein receptor family. J Thromb Haemost 2006;4:1680–90.

47 Andersen OM, Benhayon D, Curran T *et al.* Differential binding of ligands to the apolipoprotein E receptor 2. Biochemistry 2003;42:9355–64.

48 Lutters BC, Derksen RH, Tekelenburg WL *et al.* Dimers of beta 2-glycoprotein I increase platelet deposition to collagen via interaction with phospholipids and the apolipoprotein E receptor 2′. J Biol Chem 2003;278:33831–8.

49 van Lummel M, Pennings MT, Derksen RH *et al.* The binding site in β2-glycoprotein I for ApoER2′ on platelets is located in domain V. J Biol Chem 2005;280:36729–36.

50 Bohgaki M, Matsumoto M, Atsumi T *et al.* Plasma gelsolin facilitates interaction between beta2 glycoprotein I and alpha5beta1 integrin. J Cell Mol Med 2011;15:141–51.

51 Marai I, Carp H, Shai S *et al.* Autoantibody panel screening in recurrent miscarriages. Am J Reprod Immunol 2004;51: 235–40.

52 Sugiura-Ogasawara M, Atsumi T, Ozaki Y *et al.* Phosphatidylserine-dependent antiprothrombin antibodies are not useful markers for high-risk women with recurrent miscarriages. Fertil Steril 2004;82:1440–2.

53 Yamada H, Atsumi T, Kobashi G *et al.* Antiphospholipid antibodies increase the risk of pregnancy-induced hypertension and adverse pregnancy outcomes. J Reprod Immunol 2009;79:188–95.

Lupus (2013) 22, 761–771
http://lup.sagepub.com

PAPER

The involvement of CD36 in monocyte activation by antiphospholipid antibodies

M Kato, T Atsumi, K Oku, O Amengual, H Nakagawa, Y Fujieda, K Otomo, T Horita, S Yasuda and T Koike
Department of Medicine II, Hokkaido University Graduate School of Medicine, Sapporo, Japan

Background: CD36, known as a scavenger receptor, is a transmembrane glycoprotein expressed on monocytes, platelets and endothelial cells, recognizes multiple ligands, including phosphatidylserine, and regulates atherogenesis and thrombosis. The objective of this study is to investigate the possible involvement of CD36 in the pathophysiology of thrombosis in patients with antiphospholipid syndrome (APS). **Methods:** First, rs3765187, a missense mutation linked to CD36 deficiency, was investigated by TaqMan polymerase chain reaction (PCR) genotyping method in 819 Japanese, including 132 patients with APS, 265 with systemic lupus erythematosus (SLE) in the absence of APS, and 422 healthy subjects. Then, the involvement of CD36 in antiphospholipid antibody (aPL)-induced tissue factor (TF) expression was examined using CD36-null mice or anti-CD36. Purified IgG from patients with APS and a monoclonal phosphatidylserine-dependent antiprothrombin antibody were used in these experiments. TF expression was tested by real-time PCR and flow cytometry. **Results:** Minor allele carrier of rs3765187 was less frequent in patients with APS (3.8% $p=0.032$), but not in patients with SLE in the absence of APS (7.9% $p=0.32$), compared with healthy subjects (10.2%). The aPL-induced TF expression was significantly suppressed on peritoneal macrophages from CD36-null mice compared to wild type and significantly inhibited by anti-CD36 on human monocytes. **Conclusions:** The gene mutation linked to CD36 deficiency was less frequent in patients with APS. The deficient or suppressed CD36 function significantly reduced aPL-induced TF expression in vitro. Taken together, in a susceptible background CD36 scavenger receptor function may be involved in the thrombotic pathophysiology in patients with APS. *Lupus* (2013) **22,** 761–771.

Key words: Antiphospholipid syndrome; lupus anticoagulant; thrombosis; scavenger receptor

Introduction

Antiphospholipid syndrome (APS) is an autoimmune disorder in which vascular thrombosis or pregnant morbidity occurs in patients having persistent laboratory evidence of antiphospholipid antibodies (aPL). It correlates with a poor prognosis or impaired activity of daily living for a high relapse rate of thrombosis.[1]

Pathogenic aPL contains β2 glycoprotein I-dependent anticardiolipin antibodies (aCL/β2GPI) and phosphatidylserine-dependent antiprothrombin antibodies (aPS/PT).[2,3] Both antibodies recognize epitopes on the phospholipid-binding proteins (β2GPI or prothrombin) interacting with negatively charged phospholipids, such as cardiolipin and phosphatidylserine. It is commonly believed that these epitopes express only when the phospholipid-binding proteins bind with anionic phospholipids.[4] In the 1990s, the function of phospholipid-binding protein was extensively studied based on the hypothesis that the interaction of aPL with their antigens impairs their anti- or procoagulant activities. However, the activation of procoagulant cells (monocyte, endothelial cell and platelet) through the binding of phospholipid-binding protein and aPL has been the focus of investigations during the last decade.[1]

Tissue factor (TF) upregulation has been advocated as one of the most important mechanisms in the pathogenesis of APS. Monocytes and endothelial cells treated with aPL demonstrate upregulation of TF expression and function, which is accompanied by an increase in interleukin (IL)-6

Correspondence to: Tatsuya Atsumi, MD, PhD, Department of Medicine II, Hokkaido University Graduate School of Medicine, N15W7, Kita-Ku, Sapporo 060-8638, Japan.
Email: at3tat@med.hokudai.ac.jp
Received 3 December 2012; accepted 20 April 2013

10.1177/0961203313490242

or other proinflammatory substances.[5,6] Enhanced TF expression has been observed in healthy monocytes incubated with polyclonal or monoclonal aPL.[6] The activation of nuclear factor-κB (NF-κB) and p38 mitogen-activated protein kinase (MAPK) has been recognized as participating in this process as intracellular signaling pathways.[7,8] However, cell surface receptor participation in this process is still controversial, and a number of candidates have been reported, including annexin A2, apolipoprotein E receptor 2', glycoprotein Ibα, low-density lipoprotein (LDL) receptor-related protein, megalin, toll-like receptor (TLR)2, TLR4, very-low-density lipoprotein, P-selectin glycoprotein ligand-1 and integrin α5β1.[9–16]

CD36, known as a member of class B scavenger receptors, is an 88-kDa transmembrane glycoprotein expressed on monocytes, macrophages, platelets and capillary endothelial cells, residing in lipid raft domains.[17,18] CD36 recognizes multiple ligands, including anionic phospholipids, oxidized LDL, long-chain fatty acid, collagen, thrombospondin-1 and malaria-infected erythrocytes and plays a role as a mediator of multiple functions including inflammation, atherogenesis and thrombosis through the activation of p38 and JNK MAPK and NF-κB.[18,19] Human CD36 deficiency was first described in 1989 in subjects refractory to human leukocyte antigen (HLA)-matched platelet transfusions[20] and is found in 4% to 10% of Asian or African populations.[21–23] It is divided into two subgroups: In type I deficiency, neither monocyte nor platelet expresses CD36, while in type II deficiency monocyte CD36 is expressed in the absence of platelet CD36.[24] There are three major polymorphisms on the exons of CD36 gene: a missense mutation linked to human CD36 deficiency in the Japanese population (rs3765187, C478T, Pro90Ser),[21] a nonsense mutation linked to human CD36 deficiency in the African population (rs3211938, T1264G),[25] and a mutation on the 5' untranslated region (rs1049654) whose clinical significance is unknown. Some clinical phenotypes of CD36 deficiency have been reported, including hypertrophic cardiomyopathy, hypertension and dyslipidemia.[26–28] The phenotypes of CD36 knock-out (KO) mice have been reported to be protective for atherosclerosis, thrombosis and inflammation, but susceptible to infection.[19,29–31]

Considering the distribution, ligands and function of CD36, we hypothesized that CD36 is involved in the pathogenesis of APS as one of the surface receptors on procoagulant cells, and thus performed a genetic and molecular-biologic investigation.

Material and methods

Patients

A total of 819 Japanese subjects, including 132 patients with APS, 265 with systemic lupus erythematosus (SLE) in the absence of APS and 422 healthy subjects, were enrolled. All the patients fulfilled the Sydney-revised Sapporo criteria of APS[32] and/or the American College of Rheumatology classification criteria of SLE.[33] Profiles of the patients with APS are shown in Table 1. This study was performed in accordance with the Declaration of Helsinki and the Principles of Good Clinical Practice. Approval was obtained from the local ethics committee and informed consent was obtained from each study subject before enrollment.

Determination of aPL

Two clotting tests were performed for lupus anticoagulant (LA) determination, using a semiautomated hemostasis analyzer (STart 4; Diagnostica Stago, Asnières-sur-Seine, France) according to the guidelines recommended by the Subcommittee on Lupus Anticoagulant/Antiphospholipid Antibody of the Scientific and Standardisation Committee of the International Society on Thrombosis and Haemostasis.[34] For measurement of the activated partial thromboplastin time (APTT), a sensitive reagent with a low phospholipid concentration (test PTT-LA; Diagnostica Stago) was used for screening, and the results were confirmed with the use of a StaClot LA kit

Table 1 Profiles of patients with APS

Total number		*132*
Age (year)		42 (15–74)
Female		111
Primary APS		61
Complicated SLE		71
Clinical manifestations (overlapping)		
	Arterial thrombosis	83
	Venous thrombosis	43
	Pregnant morbidity	38
Autoantibodies (overlapping)		
	LA	107
	aCL	73
	aβ2GPI	66
	aPS/PT	92

APS: antiphospholipid syndrome; SLE: systemic lupus erythematosus; LA: lupus anticoagulant; aCL: anticardiolipin antibodies; aβ2GPI: anti-β2 glycoprotein I antibodies; aPS/PT: phosphatidylserine-dependent antiprothrombin antibodies.